Bone Marrow-Derived Mesenchymal Stromal Cells Enhance Chimeric Vessel Development Driven by Endothelial Cell-Coated Microtissues

Michael Dean Chamberlain, Ph.D., Rohini Gupta, Ph.D., and Michael V. Sefton, Sc.D.

Adding bone marrow-derived mesenchymal stromal cells (bmMSCs) to endothelialized collagen gel modules resulted in mature vessel formation, presumably caused in part by the observed display of pericyte-like behavior for the transplanted GFP$^+$ bmMSCs. A previous study determined that rat aortic endothelial cells (RAECs) delivered on the surface of small (~ 0.8 mm long $\times 0.5$ mm diameter) collagen gel cylinders (microtissues, modular tissue engineering) formed vessels after transplantation into immunosuppressed Sprague-Dawley (SD) rats. Although the RAECs formed vessels in this allogeneic transplant model, there was a robust inflammatory response and the vessels that formed were leaky as shown by microcomputed tomography (microCT) perfusion studies. *In vitro* assays showed that SD rat bmMSCs embedded into the collagen gel modules increased the extent of EC proliferation and enhanced EC sprouting. *In vivo*, although vessel number was not affected, the new vessels formed by the bmMSCs and RAECs were more stable and leaked less in the microCT perfusion analysis than vessels formed by implanted RAECs alone. Addition of the bmMSCs also decreased the total number of CD68$^+$ macrophages that infiltrated the implant and changed the distribution of CD163$^+$ (M2) macrophages so that they were found within the newly developed vascularized tissue. Most interestingly, the bmMSCs became smooth muscle actin positive and migrated to surround the EC layer of the vessel, which is the location typical of pericytes. The combination of these two effects was presumed to be the cause of improved vascularity when bmMSCs were embedded in the EC-coated modules. Further exploration of these observations is warranted to exploit modular tissue engineering as a means of forming large vascularized functional tissues using microtissue components.

Introduction

CURRENTLY, ONE OF THE MAIN obstacles for tissue engineering is the development of large implantable tissues with blood vessels that quickly anastomose with the vasculature of the host. To address this issue, we are exploiting the concept of modular tissue engineering, wherein modular units ("microtissues") are designed and then mixed together to form a functional organ. Simple base units are mixed together in appropriate ratios and patterns to develop complex, vascularized tissues in a bottom-up fashion. The base units used to build these complex tissues are small (here, ~ 0.8 mm long $\times 0.5$ mm diameter) cylinders made from collagen gels, called modules or "microtissues," and seeded with endothelial cells (ECs).[1,2] These modules have cells embedded in them and are then coated with ECs. Each of these modules are small enough to allow nutrient and oxygen diffusion, and several hundred modules can be im-

planted or injected where they pack together to form a large space filling tissue that is perfusable via the EC-lined channels.[3] There are two general types of modules that can be formed depending on the type of cells embedded in them. Functional modules are formed with islets or hepatocytes, for example, embedded within modules, whereas support modules contain supporting cells such as smooth muscle cells[4] or mesenchymal stromal cells (MSCs). The support modules are mixed with the functional modules to improve tissue performance and integration of the tissue into the host.

We have previously shown that empty modules that are coated with EC formed beds of perfusable capillary-like vessels that integrated with the host vascular system in an omental pouch.[5] The EC migrated off the surface of the modules and formed chimeric vessels that contained both host and implanted ECs by day 7. These vessels persisted for 60 days (longest time point measured). However, these blood vessels were slow to mature and by day 60, although there

had been a large decrease in the size of the blood island that had formed soon after implantation, the vessels were still leaky as seen by microcomputed tomography (microCT) images. This suggests that the blood vessels that formed would not be sufficiently mature to support the nutrient requirements of the functional cells. When islets were implanted using the modular system, it took approximately 21 days before the implanted islets normalized blood glucose levels.[6] We presumed that this was due to the slow development of the vascular system and that engraftment would be enhanced by improving the vasculature in the implant.

Bone marrow-derived MSCs (bmMSCs) have been known to improve the function of several tissues after ischemic injury. For example, after intravenous injection into a myocardial infarct, bmMSCs improved cardiac function by differentiating into cardiac tissue and ECs, which decreased the size of the infarct area and improved cardiac output.[7] Also, intravenous injection of bmMSCs decreased the leakiness of the blood–brain barrier after a stroke by improving EC function and vessel stability.[8] These cells participate in the healing of damaged tissue by differentiation into the appropriate cells or by paracrine effects that improve the healing environment. Such cells differentiate into several cell types including fat, bone, and cartilage.[9] Perhaps more importantly, bmMSCs exhibit trophic effects such as secreting cytokines and growth factors that modulate the inflammatory/immune system and protect hypoxic cells from apoptosis.[10,11] The growth factors and cytokines that the bmMSCs secrete affect many stages of blood vessel development, not surprisingly because bmMSCs appear to be of similar origins to pericytes, which are associated with blood vessels.[12,13] In several studies, bmMSCs have been shown to secrete collagen, fibronectin, fibroblast growth factor, interleukin (IL)1β, IL6, IL8, IL11, leukocyte migration inhibitory factor, macrophage colony-stimulating factor, macrophage migration inhibitory factor, platelet-derived growth factor (PDGF), stromal cell-derived factor 1, transforming growth factor (TGF)β2, tissue inhibitor of metalloproteinases (TIMP)1, TIMP2, and vascular endothelial growth factor (VEGF).[14] Several groups have added MSCs to implanted tissue to stabilize vascular constructs in severe combined immunodeficiency (SCID) mice models wherein few vessels form without support.[15–17] In these cases, the addition of MSCs stabilized the newly forming vessels via direct interaction, but no vessels formed when ECs were implanted alone.[16]

We extend these prior studies to the immunosuppressed outbred Sprague-Dawley (SD) rat and show that the bmMSCs have important roles in an omental pouch model, where an initial vascular system was formed (albeit slowly) without the addition of support cells or transfection of the ECs with stabilizing genes.[5] To the best of our knowledge, this is the first study to determine the response of MSCs in a model system where they are not absolutely required for the formation of blood vessels from the implanted ECs. This system then allows us to explore what happens to the MSCs as the blood vessels mature beyond their role in vessel formation. This study also extends prior studies by determining the amount of host vessels that penetrate into the artificial construct as well as the vessels that form from the implanted ECs, as both vessel types ultimately form the vascular of the implant, and examining the effect of the implanted MSCs on the host inflammatory response to the transplanted artificial

tissue. As this was an allogeneic transplant, the rats were treated with tacrolimus and atorvastatin. Tacrolimus is an immunosuppressant and atorvastatin enhances the survival of the allogeneic ECs.[5] The bmMSCs were embedded into the collagen modules that were coated with ECs and implanted into the SD rats. The formation and maturation of the blood vessels that developed in the implanted tissue was then assessed over a 21-day period.

Materials and Methods

Cells

SD rat aortic ECs (RAECs) were purchased from VEC Technologies (Rensselaer, NY) and maintained in MCDB-131 complete medium (VEC Technologies) with 10% fetal bovine serum (FBS) at 37°C and 5% CO_2. Cells were used between passages 3 and 5. In some cases, RAECs were stably transduced with an HIV-1-based recombinant lentivirus encoded for enhanced green fluorescent protein (GFP), as previously described.[5]

BmMSC isolation

BmMSCs were harvested from SD rats as outlined by Lennon and Caplan.[18] Briefly, the femur and tibia were removed from the hind legs of the rat and cleaned of all muscle and connective tissue. The head of the femur was cut off below the lesser trochanter and the malleolus of the tibia was cut off at the fusion point of the fibula with the tibia. Holes were then drilled into the bones using an 18G needle at the supracondylar area of the femur and the tibial plateau of the tibia. The bone marrow was flushed out of the bones by inserting an 18G needle into the bones and passing 10 mL of Dulbecco's modified Eagle's medium (DMEM) through the bones several times. The collected cells were plated on non-tissue culture polystyrene at a density of 9×10^5 cells/cm^2 in DMEM supplemented with 10% FBS. Medium was changed every 3–4 days and the cells were passaged after colonies had developed, which takes about 14 days. The bmMSCs were used under passage 5. In some cases, bmMSCs were isolated from GFP SD rats (RRRC, Columbia, MO).

Module fabrication

Type 1 bovine collagen (3.1 mg/mL; Cohesion Technologies, Palo Alto, CA) modules (∼2 mm long × 0.6 mm diameter) were prepared as previously described.[3,19,20] BmMSCs were suspended in the collagen at a concentration of 1.0×10^6 cells/mL. RAECs (2.5×10^6) were seeded dynamically onto the surface of 1 mL of modules (produced using 2.5 m of tubing) for 45 min on a low-speed shaker and incubated for 7 days prior to implantation. RAECs contracted collagen modules to ∼0.8 mm long × 0.5 mm diameter. The modules were grown in a 1:1 blend of DMEM and MCDB-131 complete medium supplemented with 10% FBS and 1% pencillin-streptomycin (P/S). This medium did not cause the bmMSCs to differentiate and allowed the confluent RAECs to form tight junctions as shown by VE-cadherin staining (data not shown).

Proliferation assay

The Alamar blue assay was performed according to the manufacturer's instructions. Briefly, RAECs (5000 cells/well)

were grown in the bottom chamber of a 6-well transchambered plate (BD Biosciences, Bedford, MA) using a 1:1 blend of DMEM and MCDB-131 complete medium supplemented with 1% FBS for 7 days. The upper chambers were either left empty or filled with bmMSCs (50,000 cells/well) in the DMEM/MCDB-131 media blend. On day 7, the upper chamber containing the bmMSCs and all of the media were removed. The bottom medium was replaced with 2 mL of fresh medium containing 10% Alamar blue (Invitrogen, Carlsbad, CA), which was incubated with the RAECs at 37°C for 3 h. The reduction of the Alamar blue was measured by absorbance at 570 nm using a reference wavelength of 600 nm. The assay was conducted in triplicate.

Angiogenesis sprouting assay

As adapted from Ref.[21], RAECs were mixed with dextran-coated Cytodex 3 microcarriers (Amersham Pharmacia Biotech, Piscataway, NJ) at 400 RAEC per bead in 1 mL of MCDB-131 complete medium plus 10% FBS (VEC Technologies). The beads and cells were shaken gently every 20 min for 4 h at 37°C. The beads and cells were then resuspended in 4 mL of MCDB-131 complete medium plus 10% FBS and transferred to a 10 cm tissue culture plate (BD Biosciences) and left overnight at 37°C. The following day, beads coated with cells were washed three times with 1 mL of medium and resuspended in 2.5 mg/mL of fibrinogen (pH 7.4; Sigma, St. Louis, MO) with 0.15 units/mL of aprotinin (Sigma) at a concentration of 200 beads/mL. Five hundred microliters of fibrinogen/bead solution was added to 0.625 units of thrombin (Sigma) in a well of a 24-well tissue culture plate. Fibrinogen/bead solution was allowed to clot for 5 min at room temperature and then at 37°C for 20 min. After the fibrin gel had formed, a 250 μL collagen gel was overlaid on top of it. The collagen gel was either empty or contained bmMSCs at a concentration of 1.0×10^6 cells/mL of collagen. The collagen was gelled at 37°C for 30 min. One milliliter of medium (50% mix of DMEM and MCDB-131 complete with 10% FBS and 1% P/S) was added to the well and the medium was changed every 2–3 days. At day 7, pictures of 25 beads per condition per replicate were taken using a Zeiss Axiovert light microscope equipped with a CCD camera. The number and length of sprouts were determined using ImageJ software (National Institutes of Health, Bethesda, MD).

Module transplants

Adult female SD rats (7 weeks of age, 250–300 g; Charles River, Wilmington, MA) were individually housed and fed ad libitum. Animals were divided into two groups: untreated and drug (tacrolimus and atorvastatin) treated. Tacrolimus (Astellas, Markham, ON) was administered intramuscularly daily (days 1–6: 0.3 mg/kg; days 7–14: 0.2 mg/kg; and days 15–21: 0.1 mg/kg) in a saline solution and atorvastatin (Pfizer, Kirkland, QC) was administered daily from the day before surgery until 21 days after surgery via oral gavage at a dose of 0.5 mg/kg in sterile water. Approximately 500 modules, suspended in 0.5 mL of phosphate-buffered saline (PBS), were implanted in an omental pouch created as previously described.[5,22] For both untreated and drug-treated groups, animals were transplanted with endothelialized modules for 3, 7, 14, and 21 days ($n = 5$). The

study was approved by the University of Toronto Animal Care Committee.

Perfusion studies

Animals were heparinized (500 units; LEO Pharma, Inc., Thornhill, ON) 5 min prior to the procedure by subcutaneous injection. Following a published protocol,[23] the descending aorta was cannulated and heparinized PBS (5 U/mL) was perfused at a constant pressure of 100 mmHg until the blood was flushed from the vascular system. Animals were then perfused with 25 mL of Microfil® solution (MV-122; Flow-Tech, Carver, MA). The Microfil solution was allowed to polymerize for at least 90 min and then the omental tissue was excised into 4% formalin (Sigma Aldrich, Oakville, ON) and embedded in 1% agar solution and images were obtained with a General Electric Medical Systems MS8 microCT at the MiCE imaging facility (Toronto Institute for Phenogenomics).

Histology and immunostaining

Animals were sacrificed and the omental pouch was excised into 4% neutral buffered formalin and fixed for 48 h. Tissue samples were embedded in paraffin and 4 μm sections were cut at three levels that were 100 μm apart. Sections were processed and stained for Masson's trichrome (Fisher, Ottawa, ON) and various antibodies: Bandeiraea Simplicifolia Lectin 1 (BS-1; 1:300 dilution; Vector Laboratories, Burlingame, CA), CD68 (1:600 dilution; MCA341, AbD Serotec, Raleigh, NC), CD163 (1:500 dilution; MCA342, AbD Serotec), GFP (1:3000; AB6556, Abcam, Cambridge, MA), smooth muscle α-actin (SMA; 1:1000 dilution; AB5694, Abcam), and Von Willebrand factor (vWF; 1:5000 dilution; CL20176A-R, Cedarlane, Burlington ON). Sections were viewed with a Zeiss Axiovert light microscope equipped with a CCD camera.

Histology quantification

BS-1, a microvascular EC marker,[24] or vWF (both micro- and macrovascular ECs)-positive cells were counted using a microvessel density (MVD) method by a blinded observer as previously described.[5,22] The MVD method was applied to count BS-1 or vWF-positive vessels (with a defined lumen) at 400× magnification in three representative hot spots and the average of the three MVD counts was used for statistical analysis. Macrophages (CD68 positive) were counted in five representative sections at a magnification of 400 times and the average of these counts was used for statistical analysis. GFP vessels were counted in one section of the whole omentum tissue. The whole microscope slide (stained with GFP) was digitized using the Aperio ScanScope XT and cross-sectional diameter of each GFP vessel was measured manually in the Aperio ImageScope software (Vista, CA). Vessels were then binned according to size ranges as either capillaries (1–9 μm), small arterioles/venules (9–15 μm), large arterioles/venules (15–75 μm), or abnormal (>75 μm).

Statistical analysis

A one-way analysis of variance with Tukey's *post hoc* analysis was applied to compare means between multiple groups. Data were considered statistically significant at

$p < 0.05$. All analysis was done with GraphPad Prism software (GraphPad, La Jolla, CA).

Results

The effect of bmMSCs on EC proliferation (Fig. 1A) and EC sprouting (Fig. 1B–D) was assessed. The presence of bmMSCs in a transwell plate increased the number of ECs, as measured by Alamar blue reduction after 7 days, indicating that the bmMSCs influenced EC proliferation through paracrine effects (Fig. 1A). In the sprouting assay, coculture with bmMSCs increased the number and length of tube-like sprouts formed by the ECs on Cytodex 3 beads after 7 days (Fig. 1B, C, D).

Modules containing bmMSCs and coated with RAECs were implanted into an omental pouch formed in an SD rat. The rats were either treated with drug (tacrolimus and atorvastatin) or not and the resulting blood vessel formation was compared with empty modules coated with ECs at days 3, 7, 14, and 21.
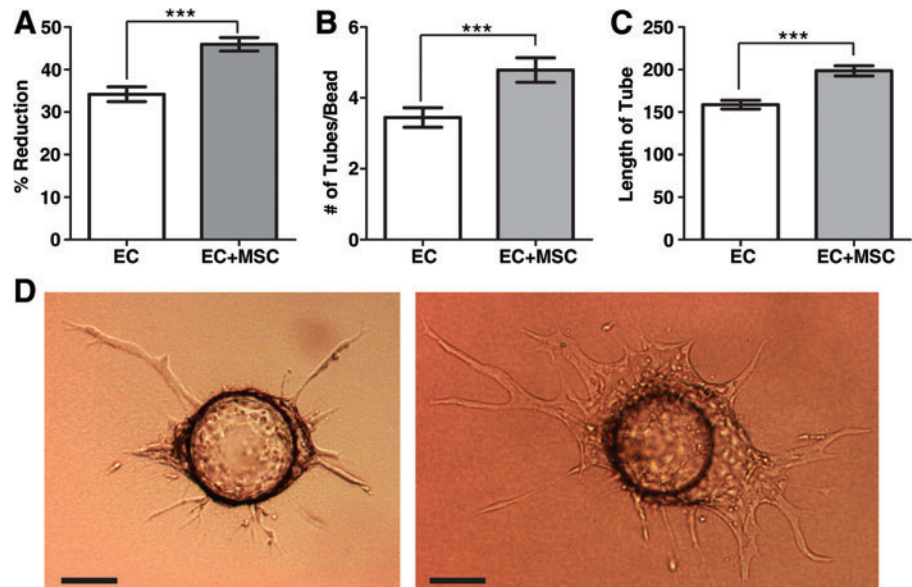
The implanted bmMSCs decreased the number of CD68^{+} macrophages in the drug-treated animals by day 14 and in the untreated animals by day 21 (Fig. 2A), consistent with literature reports of the anti-inflammatory properties of bmMSCs.[25–30] The drug treatment also decreased the number of CD68^{+} macrophages over time and the effect of the bmMSCs and drug treatment appeared to be synergic at days 14 and 21 (Fig. 2A). That the drug treatment decreased the number of CD68^{+} macrophages in the implanted tissue was previously seen in the absence of the bmMSCs.[5] In the absence of the drugs, the addition of bmMSCs did not increase EC survival past 7 days; the same poor survival was seen without bmMSCs and without the drugs (data not shown). Hence, only the effect of bmMSCs in drug-treated animals is reported.

To further characterize the infiltrating macrophages, histology sections were stained for CD163 (Fig. 2B). CD163 is a marker of the pro-angiogenic M2 macrophage subpopulation.[31] It is a haptoglobin:hemoglobin complex scavenger receptor that decreases the hemoglobin inflammatory signal by reducing the amount of free hemoglobin in a wound and its activation increases the secretion of IL-6 and IL-10, nitric oxide, IL-1β, and tumor necrosis factor-α (TNF-α).[32] The addition of bmMSCs to the implanted modules changed the distribution of the CD163^{+} macrophages in the newly formed tissue. With bmMSCs the CD163^{+} cells were found throughout the implanted tissue, whereas without the bmMSCs the CD163^{+} cells were found only at the perimeter of the implant (Fig. 2B). This difference in CD163^{+} cell distribution was maintained throughout the 21 days of this study (Fig. 2B). The CD68^{+} macrophages were evenly distributed throughout all of the implanted tissue regardless of the addition of bmMSCs (Fig. 2C), which shows that bmMSCs change the distribution of only the CD163^{+} M2 macrophages (Fig. 2B).

The decrease in the host inflammatory response and increased infiltration of the M2 macrophages did not translate into an increase in total blood vessel numbers (host and implanted) as shown by hotspot MVD counts (Fig. 3). There was no difference in counts with either BS-1, a marker of microvascular vessels, or vWF, a marker of macrovascular vessels (Fig. 3A, B). These stains stain blood vessels that develop from both host and donor ECs. There was, however, an increase in the number of chimeric blood vessels formed from the implanted ECs by day 14 as shown by a count of the chimeric vessels that contained one or more GFP[+] ECs (Fig. 3C). This means there was no change in the overall blood vessel density, but the percentage of the overall vessels that were chimeric increased. There was a small difference in the size distribution of the newly formed GFP[+] vessels, with about 10% more capillary-sized vessels at days 14 and 21 with the addition of bmMSCs to the implant (Fig. 3D). This suggests that the bmMSCs were stabilizing the developing chimeric blood vessels. Also, at day 14, the larger GFP[+] EC vessels had a better developed smooth muscle layer

FIG. 1. *In vitro* effects of bmMSCs on ECs. **(A)** Alamar blue proliferation assay. ECs (5000 cells, subconfluent) were grown in the bottom chamber of a six-well transchamber plate, with (white bar) or without (gray bar) 50,000 bmMSCs in 50% DMEM and 50% MCDB-131 plus 1% FBS for 7 days. Increased Alamar blue reduction indicated increased cell number with bmMSCs ($n = 3$; ***$p < 0.001$). **(B)** The number of sprouts or **(C)** the length of sprouts in arbitrary units that formed from the ECs (on Cytodex 3 beads) after 7 days (50% DMEM and 50% MCDB-131 plus 1% FBS) in fibrin gel overlaid with a collagen gel that was either empty (white bar) or contained bmMSCs (1.0×10^6 cells/mL, gray bar). Sprouting was increased with bmMSCs (±SEM, $n = 3$; ***$p < 0.001$). **(D)** Typical images of EC-coated bead without bmMSCs in collagen gel (left) or with bmMSCs (right) after 7 days. Scale bar is 100 μm. bmMSCs, bone marrow-derived mesenchymal stromal cells; ECs, endothelial cells; DMEM, Dulbecco's modified Eagle's medium; FBS, fetal bovine serum; SEM, standard error of the mean. Color images available online at www.liebertonline.com/tea
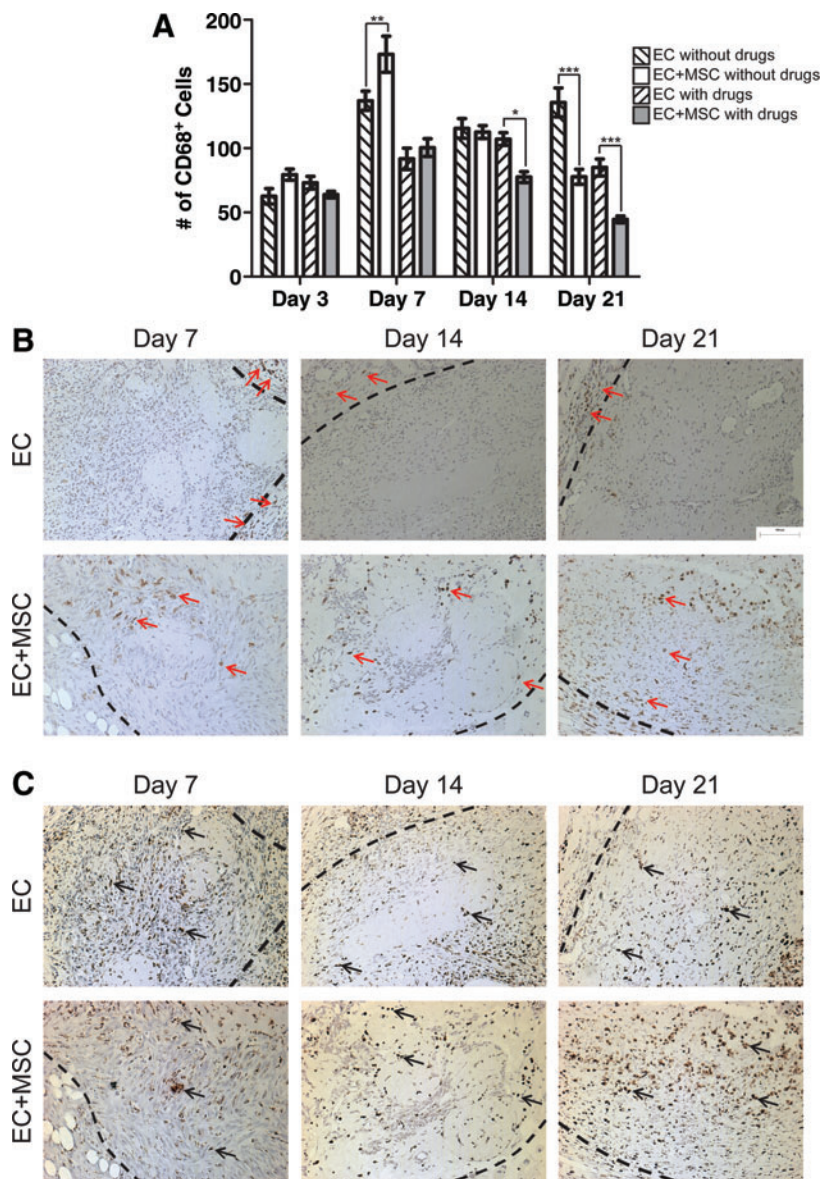
FIG. 2. The effects of bmMSCs on the inflammatory response. **(A)** CD68$^+$ macrophage counts. With drug treatment, the addition of the bmMSCs (gray bars) to the modules decreased the number of CD68$^+$ macrophages by day 14 when compared with EC modules alone (/ hashed bars). Without drug treatment, the embedded bmMSCs (white bars) had no effect on the number of CD68$^+$ macrophages when compared with EC modules alone (\ hashed bars) at day 14, but did lower the number of CD68$^+$ cells at day 21 ($\pm$SEM, $n = 5$ animals per group; *$p < 0.05$; **$p < 0.01$, ***$p < 0.001$). **(B)** The distribution of CD163$^+$ macrophages in the tissue with drug treatment. The boundary between the normal host tissue and the tissue that formed at the site of implant is shown by a dashed line. The top panels show the tissue that formed when ECs alone were implanted without bmMSCs: CD163$^+$ cells were only found on the outside of the implanted tissue (arrows). The bottom panels show the implanted tissue that contained both ECs and bmMSCs: CD163$^+$ cells were found throughout the implanted tissue (arrows). **(C)** The distribution of CD68$^+$ macrophages in the tissue with drug treatment. The boundary between the normal host tissue and the tissue that formed at the site of implant is shown by a dashed line. The top panels show the tissue that formed when ECs alone were implanted without bmMSCs and the bottom panels show the implanted tissue that contained both ECs and bmMSCs. With and without the implanted bmMSCs, the CD68 + macrophages were evenly distributed across the tissue (arrows). Color images available online at www.liebertonline.com/tea

surrounding the vessels when the bmMSCs were co-implanted than compared with the implantation of ECs alone (Fig. 4). This is shown by the well-structured architecture of the SMA-positive cell layer that is surrounding the vessels with the addition of the bmMSCs to the implant, which was not seen in the cases where the bmMSCs were not added (Fig. 4). The SMA-positive cells that were associated with the blood vessels formed a well-ordered single layer with well-defined smooth edges with the addition of the bmMSCs, similar to the architecture of a normal vessel. Without the bmMSCs, there are SMA-positive cells associated with the blood vessels, but they did not form a seemingly well-organized single layer with a smooth well-defined edge.

Although there was little difference in vessel number and size distribution, the microCT analysis showed that the addition of the bmMSCs improved the vessel integrity (consistent with the smooth muscle layer seen in Fig. 4) as there was no accumulation of microfil in the core of the implant as seen without bmMSCs (Fig. 5).
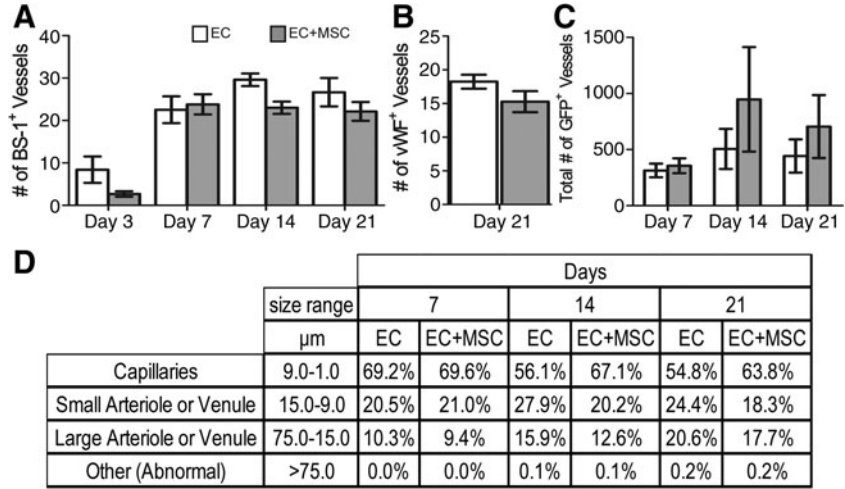
Using GFP$^+$ bmMSCs to track bmMSC migration, at day 3 the bmMSCs were inside the implanted modules (Fig. 6). By day 7, the bmMSCs migrated out of the modules and into the surrounding tissue but most were not associated with blood vessels (Fig. 6). The bmMSCs began to associate with blood vessels to a greater degree at day 14 and by day 21 most of the bmMSCs were associated with vessels (Fig. 6). The GFP$^+$ bmMSCs started to express SMA at day 7 (Fig. 7). The bmMSCs that associated with the blood vessels (starting at day 7) were SMA$^+$ and differentiated into smooth muscle-like cells (Fig. 7). There was also an overall reduction in number of MSCs over time (Fig. 6).

Discussion

The *in vitro* experiments showed that bmMSCs had a beneficial effect on the angiogenic and proliferative abilities of the ECs (Fig. 1), consistent with the literature.[33–35] BmMSCs have been shown to promote EC sprouting *in vitro*

FIG. 3. Development of blood vessels in the implanted tissue in drug-treated animals. The average microvessel density count of BS-1$^+$ blood vessels **(A)** or vWF$^+$ vessels **(B)**. There was no difference in the average density of BS-1$^+$ or vWF+ blood vessels with (gray bars) or without (white bars) the addition of bmMSCs. The average is of three hotspots per animal and five animals per group ($\pm$SEM). **(C)** The average number of GFP$^+$ EC blood vessel. By day 14, there was an increase in the number of GFP$^+$ EC blood vessels with the addition of the bmMSCs (gray bars) when compared with the implantation of ECs (white bars) alone. The total number of GFP$^+$ EC blood vessels in one whole histological section was counted per animal and the average of five animals per group is reported ($\pm$SEM). **(D)** The size distribution of GFP$^+$ blood vessels. GFP$^+$ vessels were grouped into different categories based on their size. BS-1, Bandeiraea Simplicifolia Lectin 1; vWF, Von Willebrand factor; GFP, green fluorescent protein.


		Days					
	size range	7		14		21	
	μm	EC	EC+MSC	EC	EC+MSC	EC	EC+MSC
Capillaries	9.0-1.0	69.2%	69.6%	56.1%	67.1%	54.8%	63.8%
Small Arteriole or Venule	15.0-9.0	20.5%	21.0%	27.9%	20.2%	24.4%	18.3%
Large Arteriole or Venule	75.0-15.0	10.3%	9.4%	15.9%	12.6%	20.6%	17.7%
Other (Abnormal)	>75.0	0.0%	0.0%	0.1%	0.1%	0.2%	0.2%

by secreting VEGF.[33] Ghajar *et al.* determined that coculturing bmMSCs with ECs increased the proteolytic secretion profile of ECs and that the EC sprouting relied on membrane-type matrix metalloproteinases.[34,35] This suggested that the bmMSCs would improve the quality of the blood vessels that developed using endothelialized modules. There have been several studies that have shown that, in SCID mice, blood vessels regress without the addition of support cells such as bmMSCs or transfection of the ECs with Bcl-2.[15–17,36–42] We have previously shown that in our modular tissue engineering system there was no a priori need for support cells or transfection of the ECs for the development of blood vessels.[5] However, although the blood vessels that developed did not regress over a 60-day period, they were leaky even after 60 days.[5]

Here we have shown that the addition of bmMSCs to our implant model improved the formation of the vascular bed. The blood vessel formation was enhanced as shown by the

FIG. 4. Organization of the smooth muscle layer of GFP$^+$ EC vessels at day 14. The images are of GFP$^+$ vessels from implanted tissue with and without bmMSCs. Scale bars are 200 μm. Animals were drug treated. Serial sections were stained with trichrome, SMA, and GFP. The trichrome staining shows the collagen in green and the general architecture of the tissue. The SMA staining shows the myofibroblasts or smooth muscle cells that associate with the blood vessel and the GFP staining is the implanted ECs. The dashed box outlines the area shown as magnified images in the rows below. Scale bars of the magnified images are 50 μm. SMA, smooth muscle actin. Color images available online at www.liebertonline.com/tea
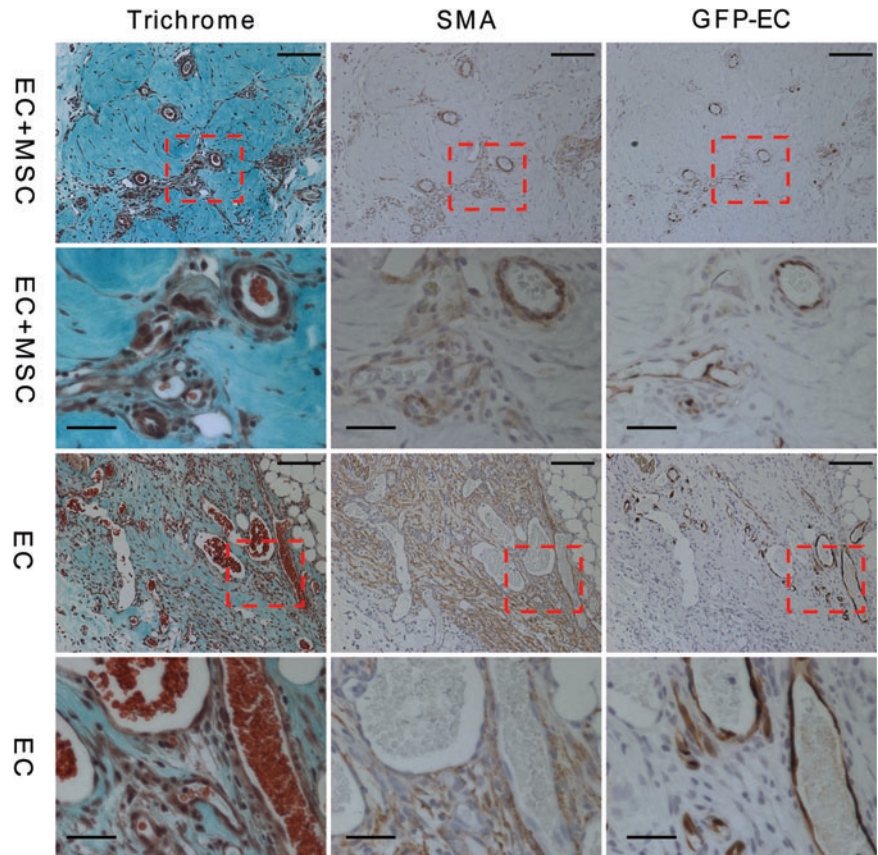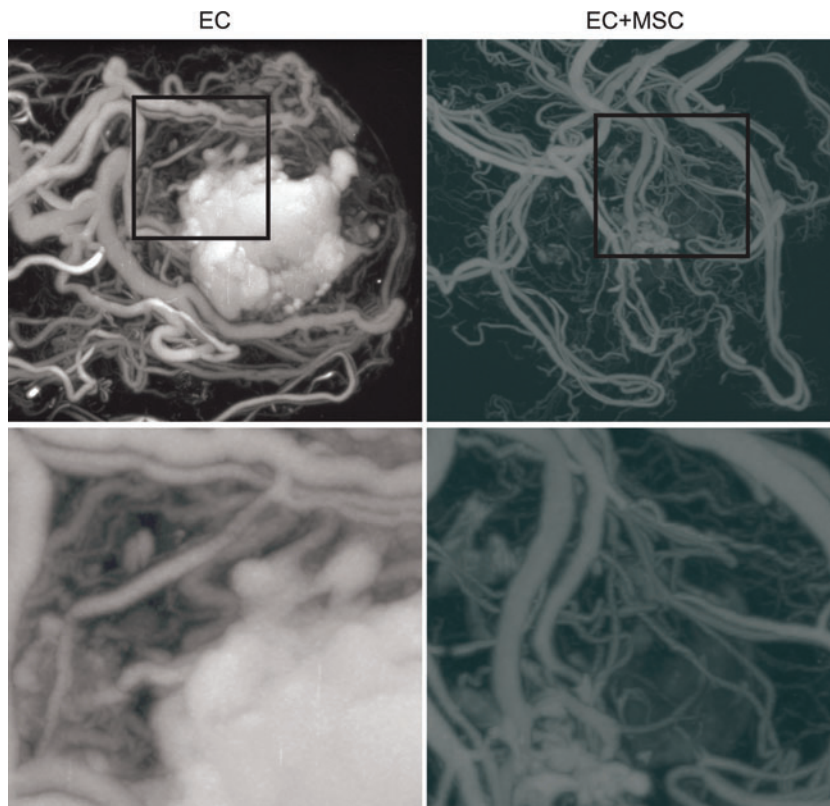
FIG. 5. MicroCT images of the implanted tissue at day 21. MicroCT images of the whole omental pouch show the vasculature of the implanted tissue. As shown in the panels on the right, the addition of bmMSCs to the implant improved the quality of the newly formed vessels as evident by the resolution of leaky core (the white microfil-rich region) when compared with the ECs alone implant (left). Animals were drug treated. MicroCT, microcomputed tomography. Color images available online at www.liebertonline.com/tea

loss of the large hematoma in the microCT perfusion images at day 21 when compared with the implantation of EC alone (Fig. 5). Also, starting at day 14 the SMA$^+$ cells surrounding the newly formed vessels were more highly ordered with the addition of the bmMSCs and formed distinct rings around the vessels, which were not seen in the ECs only condition (Fig. 4).

The improvement in blood vessel formation was presumed to be due to both the direct interactions of the bmMSCs with the newly formed blood vessels and the indirect interactions of the bmMSCs with the host. The bmMSCs migrate out of the implanted modules into the granulation tissue that formed around the implanted modules (Fig. 6). Some of the bmMSCs that migrated into this granulation tissue assumed a pericyte-like location by day 7 (Fig. 7). This association of the bmMSCs with the blood vessels increased over time (Fig. 6). There was also a colocalization of some the GFP$^+$ bmMSCs with the SMA staining (Fig. 7). This SMA staining is consistent with the notion that the bmMSCs differentiated into a pericyte-like cell type. The ability of bmMSCs, in the context of modules, to differentiate into a pericyte-like cell type has been confirmed by *in vitro* experiments, where bmMSCs become SMA and desmin positive in the presence of ECs when subject to flow in a microfluidic remodeling chamber.[43] These observations are consistent with other reports in which bmMSCs have also been shown to differentiate into both vWF$^+$ ECs and SMA$^+$ pericytes after implantation into a hind-leg ischemia model.[44]

As it has become clear that bmMSCs and perhaps almost all MSCs are normally resident as pericytes before isolation,[12,13] it is perhaps not surprising that the bmMSCs express aspects of the pericyte phenotype upon implantation with vessel-forming ECs. Also, bmMSCs have been shown to increase the density and stability of tube formation by HUVECs when they are cocultured *in vitro* by associating with the newly formed tubes.[45] The complete mechanisms of bmMSC differentiation have not been elucidated, but
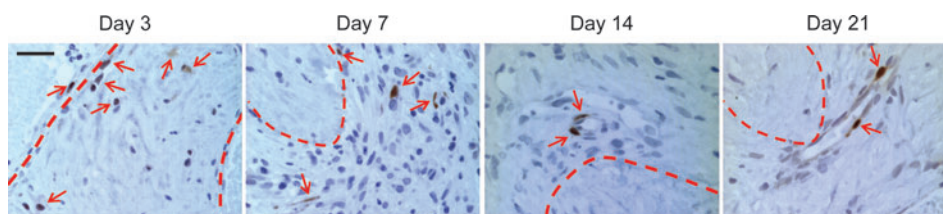

FIG. 6. Migration of GFP$^+$ bmMSCs. At day 3, the GFP$^+$ bmMSCs (arrows) were found inside the modules (dashed lines). By day 7, they migrated out of the modules into the granulation tissue that formed around the modules; few if any appeared to remain inside the modules. Some of the GFP$^+$ bmMSCs were found associated with blood vessels. At day 14, most of the GFP$^+$ bmMSCs were associated with blood vessels and by day 21 all of the GFP$^+$ bmMSCs were incorporated into the newly formed blood vessels. Animals were drug treated. Scale bar is 50 μm. Color images available online at www.liebertonline.com/tea

FIG. 7. SMA expression in GFP⁺ bmMSCs at day 7. The top panels are low-magnification images of the implanted tissue showing the tissue architecture and distribution of the GFP⁺ bmMSCs (scale bar = 400 μm). The dashed boxes in the top panels are the middle panels. The lower panels show the indicated regions (dashed box) from the middle panels (scale bar = 100 μm) at higher magnification. Several of the GFP⁺ bmMSCs colocated with cells that were SMA positive (arrows). These cells surrounded a blood vessel and were in a pericyte-like position. Animals were drug treated. Color images available online at www .liebertonline.com/tea
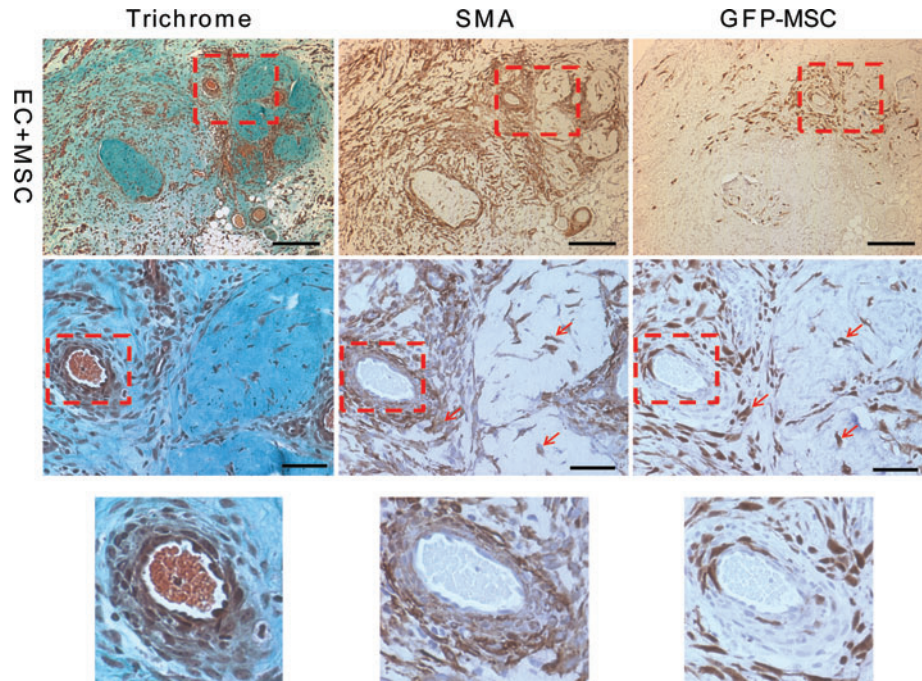
PDGF-BB is known to induce cell proliferation and migration of the mural cell precursor 10T1/2 cells[46,47] and TGF-β causes these cells to develop smooth muscle cell markers via activation of the transcription factor serum response factor.[48] Several recent studies suggest that this is because there are multiple bone marrow cell types that can differentiate into pericytes, which implies that there may be several different mechanisms for bmMSC differentiation into pericytes.[49–51] Stewart *et al.* recently reported that the differentiation of bmMSCs is in part regulated by Dll4-Notch signaling and that, by inhibiting the Dll4-Notch signaling, there was approximately a 50% decrease in the expression of pericyte markers.[52]

The bmMSCs also had indirect effects on both the ECs and the host response. The *in vitro* experiments show that the bmMSCs secrete factors that enhanced both the proliferation and angiogenesis capability of the ECs (Fig. 1). With the addition of the MSCs, there was an enhancement of donor EC (GFP⁺ EC) incorporation into the newly formed blood vessels of the implanted tissue, which increased the density of GFP⁺ vessels in the implant (Fig. 3C). This is similar to what other groups have found when human MSCs were implanted with ECs and the density of human vessels formed from implanted ECs was determined.[16,17] Interestingly and importantly, although there was an increase in the number of GFP⁺ vessels (with bmMSCs) and an enhancement of the quality of the developing blood vessels, the total number (host plus donor ECs) of blood vessels did not increase: there was no difference in vessel density with the addition of MSCs (Fig. 3A, B). This suggests that MSCs improved the survival and engraftment of donor ECs but does not result in the formation of more vessels. This observation suggests that the absolute blood vessel density of the vascularized implant is controlled by other factors when the addition of MSCs is not required for vessel formation.

The bmMSCs may increase the survival of implanted cells by altering the remodeling and host response to the im-

planted modules. The inflammatory response, as shown by macrophage infiltration, resolved faster with the addition of the bmMSCs. By day 14, there was a significant decrease in the number of infiltrating CD68⁺ macrophages with the EC and bmMSC implants when compared with the EC alone implants and the number of CD68⁺ macrophages continued to decrease at day 21 (Fig. 2). In studies of acute myocardial infarction treatment with bmMSCs, there was a decrease in pro-inflammatory cytokines, which suggests that there was also a decrease in inflammatory cells.[53] It is thought bmMSCs decrease the inflammatory response by secretion of anti-inflammatory cytokines.[54] The effect of bmMSCs on the distribution of CD163⁺ (M2) macrophages may also have benefited the survival of the implanted ECs. M2 macrophages secrete VEGF, PDGF, TNFα, and TGFβ, which improve the survival of ECs and angiogenesis.[55] BmMSCs have been shown to secrete prostaglandin E2, which transforms macrophages into an M2 phenotype.[27] Although the distinction between M1 and M2 macrophages appears to be an oversimplification,[56] the suggestion that the CD163⁺ macrophages infiltrating the implanted modules in response to the presence of bmMSCs is beneficial and worth pursuing.

Although beneficial changes to the vasculature have been shown, we have not yet demonstrated that the bmMSCs enhance the survival and function of an engineered tissue after implantation. To test this, we are developing a method of modular organ engineering where we make several different types of base units that are cultured individually *in vitro* but that are mixed together during implantation to form complex tissues. We are exploring this concept in two scenarios, using modules containing either primary hepatocytes or islets mixed with modules containing the bmMSCs.

Conclusion

The addition of bmMSCs into an endothelialized modular tissue construct improved and accelerated the quality of the

developing vascular system of the graft and ameliorated the host response to the implanted tissue.

Acknowledgments

Disclosure Statement

No competing financial interests exist.

References

1. McGuigan, A.P., and Sefton, M.V. Design and fabrication of sub-mm-sized modules containing encapsulated cells for modular tissue engineering. Tissue Eng **13,** 1069, 2007.
2. McGuigan, A.P., and Sefton, M.V. Design criteria for a modular tissue-engineered construct. Tissue Eng **13,** 1079, 2007.
3. McGuigan, A.P., and Sefton, M.V. The thrombogenicity of human umbilical vein endothelial cell seeded collagen modules. Biomaterials **29,** 2453, 2008.
4. Leung, B.M., and Sefton, M.V. A modular tissue engineering construct containing smooth muscle cells and endothelial cells. Ann Biomed Eng **35,** 2039, 2007.
5. Chamberlain, M.D., Gupta, R., and Sefton, M.V. Chimeric vessel tissue engineering driven by endothelialized modules in immunosuppressed Sprague-Dawley rats. Tissue Eng **17,** 151, 2011.
6. Gupta, R., and Sefton, M.V. Application of an endothelialized modular construct for islet transplantation in syngeneic and allogeneic immunosuppressed rat models. Tissue Eng **17,** 2005, 2011.
7. Nagaya, N., Fujii, T., Iwase, T., Ohgushi, H., Itoh, T., Uematsu, M., Yamagishi, M., Mori, H., Kangawa, K., and Kitamura, S. Intravenous administration of mesenchymal stem cells improves cardiac function in rats with acute myocardial infarction through angiogenesis and myogenesis. Am J Physiol **287,** H2670, 2004.
8. Zacharek, A., Chen, J., Cui, X., Li, A., Li, Y., Roberts, C., Feng, Y., Gao, Q., and Chopp, M. Angiopoietin1/Tie2 and VEGF/Flk1 induced by MSC treatment amplifies angiogenesis and vascular stabilization after stroke. J Cereb Blood Flow Metab **27,** 1684, 2007.
9. Caplan, A.I. Why are MSCs therapeutic? New data: new insight. J Pathol **217,** 318, 2009.
10. Caplan, A.I. What's in a name? Tissue Eng **16,** 2415, 2010.
11. Caplan, A.I., and Dennis, J.E. Mesenchymal stem cells as trophic mediators. J Cell Biochem **98,** 1076, 2006.
12. Corselli, M., Chen, C.W., Crisan, M., Lazzari, L., and Peault, B. Perivascular ancestors of adult multipotent stem cells. Arterioscler Thromb Vasc Biol **30,** 1104, 2010.
13. Crisan, M., Yap, S., Casteilla, L., Chen, C.W., Corselli, M., Park, T.S., Andriolo, G., Sun, B., Zheng, B., Zhang, L., Norotte, C., Teng, P.N., Traas, J., Schugar, R., Deasy, B.M., Badylak, S., Buhring, H.J., Giacobino, J.P., Lazzari, L., Huard, J., and Peault, B. A perivascular origin for mesenchymal stem cells in multiple human organs. Cell Stem Cell **3,** 301, 2008.
14. Zou, Z., Zhang, Y., Hao, L., Wang, F., Liu, D., Su, Y., and Sun, H. More insight into mesenchymal stem cells and their effects inside the body. Exp Opin Biol Ther **10,** 215, 2010.
15. Melero-Martin, J.M., and Bischoff, J. Chapter 13. An *in vivo* experimental model for postnatal vasculogenesis. Methods Enzymol **445,** 303, 2008.
16. Au, P., Tam, J., Fukumura, D., and Jain, R.K. Bone marrow-derived mesenchymal stem cells facilitate engineering of long-lasting functional vasculature. Blood **111,** 4551, 2008.
17. Traktuev, D.O., Prater, D.N., Merfeld-Clauss, S., Sanjeevaiah, A.R., Saadatzadeh, M.R., Murphy, M., Johnstone, B.H., Ingram, D.A., and March, K.L. Robust functional vascular network formation *in vivo* by cooperation of adipose progenitor and endothelial cells. Circ Res **104,** 1410, 2009.
18. Lennon, D.P., and Caplan, A.I. Isolation of rat marrow-derived mesenchymal stem cells. Exp Hematol **34,** 1606, 2006.
19. McGuigan, A.P., Leung, B., and Sefton, M.V. Fabrication of cell-containing gel modules to assemble modular tissue-engineered constructs [corrected]. Nature Protoc **1,** 2963, 2006.
20. Chamberlain, M.D., Butler, M.J., Ciucurel, E.C., Fitzpatrick, L.E., Khan, O.F., Leung, B.M., Lo, C., Patel, R., Velchinskaya, A., Voice, D.N., and Sefton, M.V. Fabrication of microtissues using modules of collagen gel containing cells. J Vis Exp **46,** pii 2177, 2010.
21. Nehls, V., and Drenckhahn, D. A microcarrier-based cocultivation system for the investigation of factors and cells involved in angiogenesis in three-dimensional fibrin matrices *in vitro*. Histochem Cell Biol **104,** 459, 1995.
22. Gupta, R., Van Rooijen, N., and Sefton, M.V. Fate of endothelialized modular constructs implanted in an omental pouch in nude rats. Tissue Eng **15,** 2875, 2009.
23. Marxen, M., Thornton, M.M., Chiarot, C.B., Klement, G., Koprivnikar, J., Sled, J.G., and Henkelman, R.M. MicroCT scanner performance and considerations for vascular specimen imaging. Med Phys **31,** 305, 2004.
24. Mattsson, G., Carlsson, P.O., Olausson, K., and Jansson, L. Histological markers for endothelial cells in endogenous and transplanted rodent pancreatic islets. Pancreatology **2,** 155, 2002.
25. Bartosh, T.J., Ylostalo, J.H., Mohammadipoor, A., Bazhanov, N., Coble, K., Claypool, K., Lee, R.H., Choi, H., and Prockop, D.J. Aggregation of human mesenchymal stromal cells (MSCs) into 3D spheroids enhances their antiinflammatory properties. Proc Natl Acad Sci U S A **107,** 13724, 2010.
26. Gotherstrom, C. Immunomodulation by multipotent mesenchymal stromal cells. Transplantation **84,** S35, 2007.
27. Maggini, J., Mirkin, G., Bognanni, I., Holmberg, J., Piazzon, I.M., Nepomnaschy, I., Costa, H., Canones, C., Raiden, S., Vermeulen, M., and Geffner, J.R. Mouse bone marrow-derived mesenchymal stromal cells turn activated macrophages into a regulatory-like profile. PloS One **5,** e9252, 2010.
28. Nemeth, K., Leelahavanichkul, A., Yuen, P.S., Mayer, B., Parmelee, A., Doi, K., Robey, P.G., Leelahavanichkul, K., Koller, B.H., Brown, J.M., Hu, X., Jelinek, I., Star, R.A., and Mezey, E. Bone marrow stromal cells attenuate sepsis via prostaglandin E(2)-dependent reprogramming of host macrophages to increase their interleukin-10 production. Nat Med **15,** 42, 2009.
29. Ohtaki, H., Ylostalo, J.H., Foraker, J.E., Robinson, A.P., Reger, R.L., Shioda, S., and Prockop, D.J. Stem/progenitor cells from bone marrow decrease neuronal death in global ischemia by modulation of inflammatory/immune responses. Proc Natl Acad Sci U S A **105,** 14638, 2008.

30. Yagi, H., Soto-Gutierrez, A., Navarro-Alvarez, N., Nahmias, Y., Goldwasser, Y., Kitagawa, Y., Tilles, A.W., Tompkins, R.G., Parekkadan, B., and Yarmush, M.L. Reactive bone marrow stromal cells attenuate systemic inflammation via sTNFR1. Mol Ther **18,** 1857, 2010.

31. Brown, B.N., Valentin, J.E., Stewart-Akers, A.M., McCabe, G.P., and Badylak, S.F. Macrophage phenotype and re-modeling outcomes in response to biologic scaffolds with and without a cellular component. Biomaterials **30,** 1482, 2009.

32. Van Gorp, H., Delputte, P.L., and Nauwynck, H.J. Scavenger receptor CD163, a Jack-of-all-trades and potential target for cell-directed therapy. Mol Immunol **47,** 1650, 2010.

33. Beckermann, B.M., Kallifatidis, G., Groth, A., Frommhold, D., Apel, A., Mattern, J., Salnikov, A.V., Moldenhauer, G., Wagner, W., Diehlmann, A., Saffrich, R., Schubert, M., Ho, A.D., Giese, N., Buchler, M.W., Friess, H., Buchler, P., and Herr, I. VEGF expression by mesenchymal stem cells contributes to angiogenesis in pancreatic carcinoma. Br J Cancer **99,** 622, 2008.

34. Ghajar, C.M., Blevins, K.S., Hughes, C.C., George, S.C., and Putnam, A.J. Mesenchymal stem cells enhance angiogenesis in mechanically viable prevascularized tissues via early matrix metalloproteinase upregulation. Tissue Eng **12,** 2875, 2006.

35. Ghajar, C.M., Kachgal, S., Kniazeva, E., Mori, H., Costes, S.V., George, S.C., and Putnam, A.J. Mesenchymal cells stimulate capillary morphogenesis via distinct proteolytic mechanisms. Exp Cell Res **316,** 813, 2010.

36. Allen, P., Melero-Martin, J., and Bischoff, J. Type I collagen, fibrin and PuraMatrix matrices provide permissive environments for human endothelial and mesenchymal progenitor cells to form neovascular networks. J Tissue Eng Regen Med **5,** e74, 2011.

37. Melero-Martin, J.M., De Obaldia, M.E., Allen, P., Dudley, A.C., Klagsbrun, M., and Bischoff, J. Host myeloid cells are necessary for creating bioengineered human vascular networks *in vivo*. Tissue Eng **16,** 2457, 2010.

38. Melero-Martin, J.M., De Obaldia, M.E., Kang, S.Y., Khan, Z.A., Yuan, L., Oettgen, P., and Bischoff, J. Engineering robust and functional vascular networks *in vivo* with human adult and cord blood-derived progenitor cells. Circ Res **103,** 194, 2008.

39. Enis, D.R., Shepherd, B.R., Wang, Y., Qasim, A., Shanahan, C.M., Weissberg, P.L., Kashgarian, M., Pober, J.S., and Schechner, J.S. Induction, differentiation, and remodeling of blood vessels after transplantation of Bcl-2-transduced endothelial cells. Proc Natl Acad Sci U S A **102,** 425, 2005.

40. Koike, N., Fukumura, D., Gralla, O., Au, P., Schechner, J.S., and Jain, R.K. Tissue engineering: creation of long-lasting blood vessels. Nature **428,** 138, 2004.

41. Schechner, J.S., Nath, A.K., Zheng, L., Kluger, M.S., Hughes, C.C., Sierra-Honigmann, M.R., Lorber, M.I., Tellides, G., Kashgarian, M., Bothwell, A.L., and Pober, J.S. *In vivo* formation of complex microvessels lined by human endothelial cells in an immunodeficient mouse. Proc Natl Acad Sci U S A **97,** 9191, 2000.

42. Shepherd, B.R., Chen, H.Y., Smith, C.M., Gruionu, G., Williams, S.K., and Hoying, J.B. Rapid perfusion and network remodeling in a microvascular construct after implantation. Arterioscler Thromb Vasc Biol **24,** 898, 2004.

43. Khan, O.F., Chamberlain, M.D., and Sefton, M.V. Towards an *in vitro* vasculature: differentiation of mesenchymal stromal cells within an endothelial cell-seeded modular construct in a microfluidic flow chamber. Tissue Eng 2011 [Epub ahead of print]; DOI: 10.1089/ten.tea.2011.0058.

44. Al-Khaldi, A., Al-Sabti, H., Galipeau, J., and Lachapelle, K. Therapeutic angiogenesis using autologous bone marrow stromal cells: improved blood flow in a chronic limb ischemia model. Ann Thorac Surg **75,** 204, 2003.

45. Sorrell, J.M., Baber, M.A., and Caplan, A.I. Influence of adult mesenchymal stem cells on *in vitro* vascular formation. Tissue Eng **15,** 1751, 2009.

46. Hirschi, K.K., Rohovsky, S.A., Beck, L.H., Smith, S.R., and D'Amore, P.A. Endothelial cells modulate the proliferation of mural cell precursors via platelet-derived growth factor-BB and heterotypic cell contact. Circ Res **84,** 298, 1999.

47. Hirschi, K.K., Rohovsky, S.A., and D'Amore, P.A. PDGF, TGF-beta, and heterotypic cell-cell interactions mediate endothelial cell-induced recruitment of 10T1/2 cells and their differentiation to a smooth muscle fate. J Cell Biol **141,** 805, 1998.

48. Hirschi, K.K., Lai, L., Belaguli, N.S., Dean, D.A., Schwartz, R.J., and Zimmer, W.E. Transforming growth factor-beta induction of smooth muscle cell phenotpye requires transcriptional and post-transcriptional control of serum response factor. J Biol Chem **277,** 6287, 2002.

49. Reddy, K., Zhou, Z., Schadler, K., Jia, S.F., and Kleinerman, E.S. Bone marrow subsets differentiate into endothelial cells and pericytes contributing to Ewing's tumor vessels. Mol Cancer Res **6,** 929, 2008.

50. Du, R., Lu, K.V., Petritsch, C., Liu, P., Ganss, R., Passegue, E., Song, H., Vandenberg, S., Johnson, R.S., Werb, Z., and Bergers, G. HIF1alpha induces the recruitment of bone marrow-derived vascular modulatory cells to regulate tumor angiogenesis and invasion. Cancer Cell **13,** 206, 2008.

51. Lamagna, C., and Bergers, G. The bone marrow constitutes a reservoir of pericyte progenitors. J Leukoc Biol **80,** 677, 2006.

52. Stewart, K.S., Zhou, Z., Zweidler-McKay, P., and Kleinerman, E.S. Delta-like ligand 4-Notch signaling regulates bone marrow-derived pericyte/vascular smooth muscle cell formation. Blood **117,** 719, 2011.

53. Tavares, A.M., da Rosa Araujo, A.S., Baldo, G., Matte, U., Khaper, N., Bello-Klein, A., Rohde, L.E., and Clausell, N. Bone marrow derived cells decrease inflammation but not oxidative stress in an experimental model of acute myocardial infarction. Life Sci **87,** 699, 2010.

54. Uemura, R., Xu, M., Ahmad, N., and Ashraf, M. Bone marrow stem cells prevent left ventricular remodeling of ischemic heart through paracrine signaling. Circ Res **98,** 1414, 2006.

55. Rodero, M.P., and Khosrotehrani, K. Skin wound healing modulation by macrophages. Int J Clin Exp Pathol **3,** 643, 2010.

56. Mosser, D.M., and Edwards, J.P. Exploring the full spectrum of macrophage activation. Nat Rev **8,** 958, 2008.

Address correspondence to:
Michael V. Sefton, Sc.D.
Department of Chemical Engineering and Applied Chemistry
Institute of Biomaterials and Biomedical Engineering
University of Toronto
164 College St., Suite 407
Toronto, Ontario
Canada M5S 3G9

E-mail: michael.sefton@utoronto.ca